Pattern formation in binary colloids

Ferenc Kun, Imre Varga

Pattern formation in binary colloids

Journal:	*Philosophical Magazine & Philosophical Magazine Letters*
Manuscript ID:	TPHM-05-Jan-0004
Journal Selection:	Philosophical Magazine
Date Submitted by the Author:	05-Jan-2005
Complete List of Authors:	Kun, Ferenc; University of Debrecen, Department of Theoretical Physics Varga, Imre; University of Debrecen, Department of Theoretical Physics
Keywords:	colloids, experimental, molecular dynamic simulations
Keywords (user supplied):	Strongly correlated electrons
Note: The following files were submitted by the author for peer review, but cannot be converted to PDF. You must view these files (e.g. movies) online.	
paper.tex figures.tgz	

Pattern formation in binary colloids

Imre Varga and Ferenc Kun*

Department of Theoretical Physics, University of Debrecen,

P. O. Box:5, H-4010 Debrecen, Hungary

(Dated: January 5, 2005)

Abstract

An experimental and theoretical study of the formation of structures in a binary monolayer of dipolar particles is presented. We construct an experimental technique for an easy to control realization of a binary monolayer where the two components have oppositely oriented dipole moments constrained perpendicular to the plane of motion. The experimental setup ensures that hydrodynamic effects do not play a crucial role in the structure formation, the particles move deterministically due to the dipole-dipole interaction. At low concentrations cluster-cluster aggregation occurs with chain-like morphologies, while at high concentration the particles self-assemble into various types of binary crystal lattices. We propose a simple theoretical framework to describe the observed structure formation. Based on molecular dynamics simulations and analytic calculations we show that the total concentration of the particles, the relative concentration and the relative dipole moment of the components determine the structure of the dipolar monolayer. The theoretical results are in satisfactory agreement with the experimental findings.

PACS numbers: 83.10.Pp, 82.70.Dd, 41.20.-q, 61.46.+w

* Electronic address:feri@dtp.atomki.hu

I. INTRODUCTION

Pattern formation by self assembly in a monolayer of colloidal particles confined to a liquid-air or liquid-liquid interface, or to the bottom plate of a container has several implications in physics, chemistry, materials science and biology. During the last few years large efforts have been devoted to the study of monolayers of particles which have a permanent dipole moment or are polarizable in an external electric or magnetic field. Investigations have been performed with several different types of particles subjected to a constant or time dependent external fields. While in the absence of an external field chains, rings and fractal clusters have been observed with a temperature dependent fractal dimension (Cernák et al. 2004, Furst and Gast 1999, 2000, Ghazali and Lévy 2003, Huang and Lai 2000, Skjeltorp 1983, Tavares et al. 2002, Teixeira et al. 2000, Weis et al. 2002, Wen et al. 1999), in the presence of an external field crystal structures emerged (Choi et al. 2000, Wen and Sheng 2003, Wen et al. 2000, Yeh et al. 1997, Zahn et al. 2003). It was demonstrated that by appropriate adjusting of the external field all the planar lattice structures can be produced (Choi et al. 2000, Froltsov et al. 2003, Terada and Tokuyama 2004, Wen and Sheng 2003, Wen et al. 2000, Yeh et al. 1997, Zahn et al. 2003), which is of high practical importance for the controlled fabrication of patterned surfaces and also addresses essential problems of statistical physics like the study of phase transitions between different morphologies and the phenomenon of melting in two dimensions (Choi et al. 2000, Wen et al. 2000, Yeh et al. 1997). For the simplest triangular lattice of dipoles the elastic properties of the crystal have also been investigated by means of video spectroscopy (Zahn et al. 2003). The study of the effect of temperature and vibrational excitations on a monolayer of magnetic particles have provided new insight into the pattern formation of dipolar systems (Blair and Kudrolli 2003, Ghazali and Lévy 2003, Strambaugh et al. 2003, Tavares et al. 2002, Teixeira et al. 2000, Weis et al. 2002). Quasi-twodimensional ordered structures have also been observed in drying liquid droplets (Helseth and Fischer 2003).

A very interesting novel type of structure formation occurs in a dipolar monolayer when the dipole moment of particles is constrained to be perpendicular to the plane of motion. The two possible orientations of the dipole moments distinguish two components of the system which can also differ in other physical properties like the magnitude of dipole moment, material type, size, mass, ... so that the system is also termed as binary colloid. A possible

physical realization of binary dipolar monolayers was recently presented in Ref. (Ristenpart et al. 2003) where particles of two different material properties were sedimented in an electro-magnetically passive liquid. The monolayer was subjected to an AC electric field perpendicular to the bottom plate of the container so that the particles attain an induced dipole moment parallel to the field. Novel behavior was obtained in the parameter range where particles of different type have oppositely oriented dipole moments attracting each other. At low concentrations binary chains, rings and polygons of alternating particles were observed, while at high concentrations the particles self assemble into binary crystal lattices (Ristenpart et al. 2003).

In this paper we present an experimental and theoretical study of the structure formation in a binary monolayer of particles. We construct an experimental method which provides a straightforward, easy to control realization of binary monolayers without an external driving field. The two components of the system are millimeter-sized particles with permanent magnetic dipole moment whose orientation is fixed to be perpendicular to the plane of motion. To decrease the frictional barrier, the particles are confined to a liquid-air interface, *i.e.* the particles float to reduce the friction with the surroundings. The setup ensures that hydrodynamic effects cannot play a crucial role, the particles undergo deterministic motion due to the dipole-dipole interaction, furthermore, the liquid makes the system over-damped. We propose a simple model of the structure formation observed in binary dipolar monolayers. Based on molecular dynamics simulations and analytic calculations we show that the total concentration of the particles, the relative concentration and the relative dipole moment of the components determine the structure of the dipolar monolayer. A satisfactory agreement is obtained between the experimental and theoretical results.

II. EXPERIMENTAL SETUP

In the experiments macroscopic metal particles of cylinder shape are magnetized along their axis. In order to facilitate the particle motion, the magnetic particles are attached to cork discs of regular shape so that the composite particle can float on the surface of a liquid. Fig. 1 illustrates that the two particles are adjusted on the top of each other to have a common axis, which ensures stability when floating. In all experiments, water was used as a carrier liquid to which a surfactant was added to reduce the surface tension. The particles are

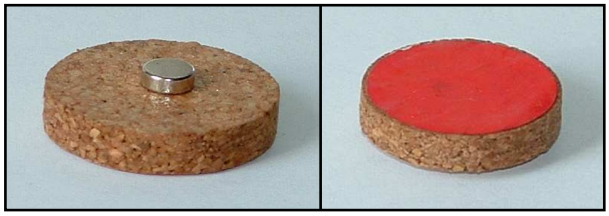

FIG. 1: (Color online) Magnetized particle attached to a cork disc of larger diameter (*left*). The composite particle can float upside down on the surface of water (*right*). The diameter d and height h values are $d = 4$ mm and $h = 1.5$ mm, and $d = 26$ mm and $h = 5$ mm, for the magnetic particle and cork disc, respectively.

placed onto the water surface with the heavier part pointing downward, *i.e.* the magnets are always under the water, see Fig. 1. In the experiments magnetic particles of three different strength were used with slightly different geometrical extensions attached always to cork discs of the same size. The cork discs have diameter $d = 26$ mm and height $h = 5$ mm, which proved to be sufficient to prevent the flipping of magnets of identical orientation in the vicinity of each other even for the largest magnetization used in the present study.

The two components of the system are realized by the two opposite orientations of the dipole moments of the particles perpendicular to the water surface. The initial state is prepared such that the particles are placed into a square shaped container of side length $L = 500$ mm when the container contained no or only a thin layer of water not enough to float the particles. The initial particle positions had been generated beforehand by a computer program and the particles were positioned by hand accordingly making use of a centimeter grid under the transparent container (see Fig. 2). The free side of the cork discs is colored according to the orientation of the dipole moments of the magnetic particles, *i.e.* the red color in Fig. 2 indicates dipole moment pointing upward perpendicular to the water surface, while yellow stands for downward dipoles. Starting from the random initial configuration, the water level is raised very slowly in order to ensure that all the particles start floating approximately at the same time. Then the floating particles move under the action of their mutual dipole-dipole interaction and form various structures.

The total concentration ϕ of the particles in our experimental box is defined as the

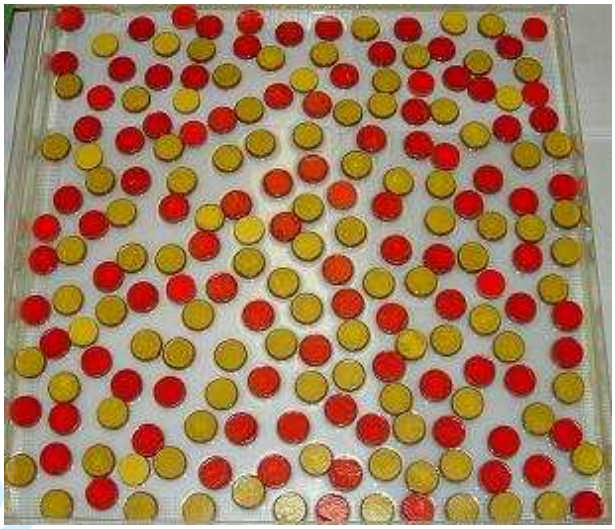

FIG. 2: (Color online) Initial configuration of 176 particles in a square box of side length $L = 500$ mm resulting in a concentration $\phi \approx 0.35$. The same amount of particles of opposite magnetic moment/different colors is used, so that $\phi_r = 1$. The water level is low enough to prevent floating of the particles.

coverage

$$\phi = \frac{NR^2\pi}{L^2}, \tag{1}$$

where N and R denote the number and radius of cork discs carrying the magnetic particles, respectively. The partial concentrations of the two components ϕ_1 and ϕ_2 can be analogously defined and their relative concentration ϕ_r follows as

$$\phi_r = \frac{\phi_1}{\phi_2}. \tag{2}$$

Experiments were performed by varying the concentration ϕ and the relative concentration ϕ_r in a broad range by controlling the number of particles N while the container size L is fixed. In contrast to previous experiments (Ristenpart et al. 2003) no external field is necessary in our setup, and the magnitude of the dipole moment is controlled by the placement of particles with the corresponding magnetization.

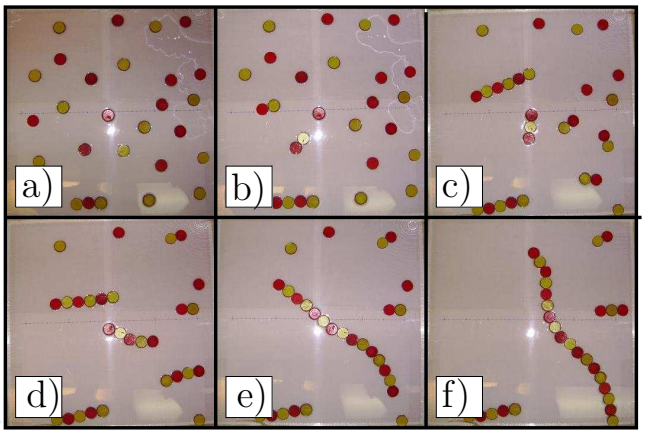

FIG. 3: (Color online) Cluster-cluster aggregation at low concentration $\phi \approx 0.05$, $\phi_r = 1$, and $\mu_r = 1$. Part of the experimental box is cut out and magnified. First single particles form short chains a, b, c), which then merge into longer chains. Snapshots taken at times $t = 1$ s (a), 10 s (b), 30 s (c), 50 s (d), 100 s (e), 200 s (f).

III. STRUCTURE FORMATION

We carried out a large amount of experiments varying the total concentration ϕ of the particles, the relative concentration ϕ_r and relative dipole moment μ_r of the components. In order to keep the particle number large even at low concentrations, a container of side length $L = 1000$ mm was also constructed, in which, for instance, the concentration $\phi = 0.05$ is realized by 102 particles.

At low concentrations we observed that due to the long range dipolar interaction, the particle system undergoes a cluster-cluster aggregation process, *i.e.* first single particles of opposite dipole orientation join and form small clusters which then further aggregate step by step until the entire system is covered by a network of particles. The time evolution of the cluster-cluster aggregation process is illustrated in Fig. 3 where part of the experimental box was cut out and magnified. The binary clusters of particles with oppositely oriented dipole moments can easily be identified in the figure. The cluster morphology is always chain-like, *i.e.* short chains merge at their ending points forming longer chains. This aggregation mechanism was found experimentally to work until the concentration is lower than $\phi^* \approx 0.1-0.15$. Above ϕ^*, due to the relatively small distance of clusters, aggregation occurs not only at chain ends but also at internal sites, making the clusters more compact with branching

morphology. Quantitative characterization of the kinetic aggregation process of the binary system can be obtained by analyzing the average cluster size and the number of clusters as a function of time, furthermore, the scaling structure of the cluster size distribution functions (Cernák et al. 2004, Skjeltorp 1983, Vicsek and Family 1984). The results will be presented in a future publication along with large scale computer simulations (Yoshioka 2005).

In the high concentration phase $\phi > \phi^*$, experiments were performed by varying the relative concentration ϕ_r and relative dipole moment μ_r of the two components. The total number of particles was fixed to 200 which provides concentration $\phi \approx 0.4$ in the box of side length $L = 500$ mm. Larger concentrations were achieved by mounting internal walls inside the container. To explore the parameter regimes of the occurrence of crystal structures, the experiments were repeated 5 times under identical conditions. A representative example of the pattern formation can be seen in Fig. 4 for a system of total concentration $\phi = 0.4$, relative concentration $\phi_r = 1$ and relative dipole moment $\mu_r = 1$. When the water level is high enough, the particles get mobilized (Fig. 4b) and rapidly aggregate into compact structures Fig. 4c). We observed that the structure of clusters is not frozen, *i.e.* due to the isotropic inter-particle forces the cluster structure is quite flexible, in contrast to particle monolayers with in-plane dipoles where the anisotropic dipolar interaction makes the clusters more rigid (Wen et al. 1999). In our case the flexibility has the consequence that when two clusters approach each other they deform facilitating the aggregation, furthermore, the subsequent aggregation steps can result in rearrangements of particles reaching deeper energy minima. Typically, the perturbation of an aggregate by a particle, joining the cluster with a non-zero velocity, may give rise to an avalanche of restructuring events. The square lattice presented in Fig. 4c) was obtained as a result of several restructurings.

Fig. 5 summarizes the crystal structures obtained experimentally in the binary monolayer. When the two components of the system have the same magnitude of dipole moment, the binary square lattice provides the deepest energy configuration (Varga et al. 2004). Experiments showed that under the condition $\phi_r = 1$, $\mu_r = 1$ the square lattice is always obtained for high enough concentrations $\phi \geq 0.4$ (see Fig. 5a). For concentrations in the interval $\phi \approx 0.2 - 0.4$, the particles form short chains which then join into a network structure with local crystalline order. It is important to emphasize that in this concentration regime, locally binary honeycomb lattice structures were obtained where particles of both types have three neighbors of opposite dipole orientation (see Fig. 5b). Our experiments showed that

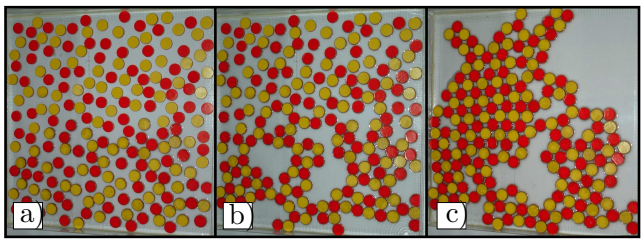

FIG. 4: (Color online) Time evolution of the pattern formation starting from an initially random configuration of 200 particles *a*). When the water level was slowly increased the particles start to move *b*) and quickly self-assemble locally into a square lattice structure *c*). The duration of the entire aggregation process was about 60 s.

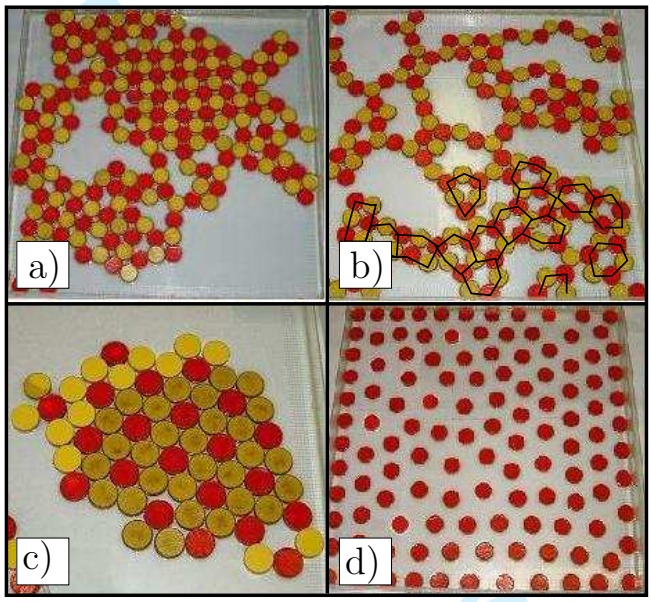

FIG. 5: (Color online) Summary of crystal structures obtained in the experiments. *a*) Square lattice occurring at $\phi_r = 1, \mu_r = 1$, and $\phi \approx 0.4$. *b*) Honeycomb lattice obtained at $\phi_r = 1, \mu_r = 1$, and $\phi \approx 0.35$. The honeycomb structure is highlighted by black lines. *c*) HCP structure at $\mu_r \approx 2.5$, and $\phi_r = 2$ obtained in a region of the container when the local concentration was about $\phi = 0.7$. *d*) Triangular lattice occurring when the system consists exclusively of one type of particles.

the binary honeycomb lattice can occur for concentrations $\phi \approx 0.3 - 0.4$ with $\phi_r = 1$ and $\mu_r = 1$.

If one of the components has a much larger magnitude of dipole moments than the other

one, binary Hexagonal Closed Packed (HCP) structure can be obtained in the limiting case of high concentrations $\phi \geq 0.7$. Such high concentrations were achieved in our experimental setup by mounting internal walls of the container. Experiments showed that very high concentrations, close to the highest coverage, are unfavorable because they freeze the particles in the initial state. The binary HCP lattice presented in Fig. 5*c*) was obtained at $\mu_r \approx 2.5$, $\phi = 0.7$. Compared to the simulation results, the concentration ϕ had to be lowered since at higher concentrations the static friction of the particles stabilized the system almost in the initial configuration. In the HCP lattice, the particles of the larger dipole moment are surrounded by 6 particles of the other type, however, only 3 particles with large dipole moment occur around the smaller one, so that the relative concentration was chosen to be $\phi_r = 2$.

If the system consists exclusively of particles of the same orientation, due to the repulsive interaction of parallel dipoles, the particles order in a triangular lattice, as illustrated in Fig. 5*d*). The particles line up along the rigid walls of the container which produces a strong distortion of the symmetry of the system so that regular triangular structures are mainly observed in the middle of the container, see Fig. 5*d*).

IV. MODEL CONSTRUCTION

In order to describe the observed structure formation, we constructed a two-dimensional dynamical model of binary dipolar monolayers. In our model an ensemble of N particles of radius R is considered in a square box of side length L on the two dimensional plane. Point-like dipole moments are assumed to be placed in the middle of the particles. The dipole moment of the particles is fixed during the time evolution of the system to be perpendicular to the plane of motion pointing either upward (particle type I) or downward (particle type II), which represents the two different material properties of the particles. The particles are considered to be suspended in an electromagnetically passive liquid so that the liquid only exerts a friction force (Stockes force) on the particles which move under the action of dipole-dipole forces. When particles touch each other during their motion we introduce a repulsive force of the form of Hertz contact to prevent the overlap (Kun et al. 2000, Luding 1998, Wen et al. 1999). After generating an initial configuration with random particle positions in the simulation box, and fixing the dipole moments according to the different material's properties, the time evolution of the system is followed by solving numerically the equation

of motion of particles for the two translational degrees of freedom with periodic boundary conditions (molecular dynamics simulation (Allen and Tildesley 1994)).

Two particles of distance r_{ij} with parallel dipole moments μ_i and μ_j exert a force onto each other of the form

$$\vec{F}_{ij}^{dd} = \frac{3\mu_i\mu_j}{r_{ij}^4}\vec{n}_{ij}, \tag{3}$$

which is isotropic (central) it always falls in the plane of motion parallel to the line $\vec{n}_{ij}$ connecting the two particles. The force is repulsive for particles of the same type and attractive for different ones. It is interesting to note that the system is rather similar to an ensemble of charges where the interaction force decreases faster than the Coulomb force. The hydrodynamic force $\vec{F}_i^{hyd}$ on a sphere is treated as Stockes's drag $\vec{F}_i^{hyd} = -\alpha\vec{v}_i$, where $\vec{v}_i$ denotes the velocity of particle i and $\alpha = 6R\pi\eta$. The particles are assumed to be deformable bodies which can overlap each other during their motion representing local deformations up to some extent. To capture the finite size of the particles, an elastic restoring force is introduced between overlapping particles according to Hertz's contact law (Luding 1998)

$$\vec{F}_{ij}^{\mathrm{pp}} = -k_{\mathrm{pp}}\left(d - r_{ij}\right)^{\frac{3}{2}} \cdot \vec{n}_{ij} = -k_{\mathrm{pp}}\vec{f}_{ij}^{\mathrm{pp}}, \tag{4}$$

where $d = 2R$ denotes the diameter of the particles, k is a material dependent constant, and the super script pp refers to the particle-particle contact. Eq. (4) expresses that the repulsive force is proportional to the 3/2 power of the overlap distance. The particle system is supposed to be fully dissipative, non-inertial, hence,

$$\begin{aligned} \frac{d\vec{r}_i}{dt} &= \frac{1}{\alpha}\sum_j \vec{F}_{ij}^{\mathrm{dd}} - \frac{k_{\mathrm{pp}}}{\alpha}\sum_{r_{ij}<2R}\vec{f}_{ij}^{\mathrm{pp}}, \\ & i = 1, \ldots, N \end{aligned} \tag{5}$$

first order differential equation system is solved numerically to obtain the trajectories of the particles (Allen and Tildesley 1994). Since no stochastic forces are introduced in the equation of motion Eq. (5), the trajectories of the particles are completely deterministic, disorder is solely introduced by the randomness of the initial configuration. In our simulations we took R, and α to be unity, and we chose k such that no significant overlap occurs.

In order to ensure the disorder of the initial configuration, first point-like particles are placed in the simulation box randomly and independently. Then the particles are gradually blown-up, *i.e.*, the particle radius is gradually increased such that after each increment

molecular dynamics simulation is performed taking into account the repulsive force arising between overlapping particles. As a results of the simulation all the particles can find an equilibrium, overlap-free position. This procedure is repeated until the particle radius R reaches the desired value.

A model system of N particles consists of N_+ and N_- particles of dipole moment μ_+ pointing upward (+), and dipole moment μ_- pointing downward (−), respectively. The concentration of particles ϕ is defined as the coverage $\phi = NR^2\pi/L^2$. The partial concentration of the two components ϕ_+, ϕ_- can be defined analogously whose ratio provides their relative concentration $\phi_r = \phi_-/\phi_+ = N_-/N_+$. In the model the magnitudes μ_+, μ_- of dipole moments can be freely varied which captures up to some extent the effect of frequency tuning in the experiment. For simplicity, we fix μ_+ and vary the ratio $\mu_r = \mu_-/\mu_+$, *i.e.* the relative dipole moment.

V. CHAINS, RINGS, AND POLYGONS

Our experiments showed that at low concentrations in the binary mixture the particles undergo a kinetic aggregation process giving rise to chains of alternating particles, furthermore, in other experiments (Ristenpart et al. 2003) closed loops of particles (rings, polygons) have also been found. The occurrence of particle rings has also been observed in magnetorheological fluids (Kun et al. 2000, Wen et al. 1999) containing particles of permanent magnetic moments and in vibrofluidized dry granular materials of dipolar particles (Blair and Kudrolli 2003, Strambaugh et al. 2003) in the absence of an external magnetic field. In these systems however, the dipolar moment of the particles lie in the plain of the ring and the anisotropic nature of the dipole-dipole interaction makes possible the ring formation: compared to a straight chain of aligned dipoles the ring is energetically favorable because the closing of the two ends of the chain overweights the energy loss due to the misalignment of dipoles (Kun et al. 2000, Wen et al. 1999).

In binary colloids, anisotropic chain-like clusters occur in spite of the isotropic interparticle forces which can be explained such that at low concentrations cluster structures are determined by the tendency that particles with parallel (oppositely) directed dipole moments try to maximize (minimize) their distance. The energy of a chain composed of an even number N of alternating particles can be written as a function of the relative dipole

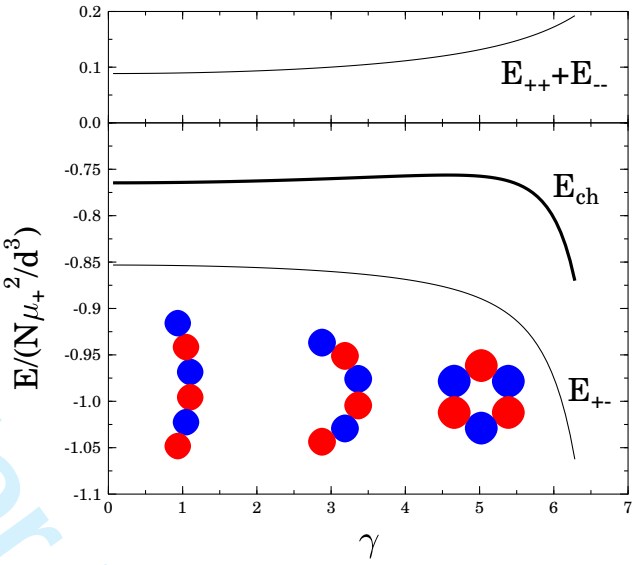

FIG. 6: Energy of a bent chain divided by the number of particles as a function of the bending angle γ obtained from Eq. (8) for $N = 6$. For clarity, the particle configurations are also shown for $\gamma = 1, \pi, 2\pi$.

moment μ_r in the form

$$E_{ch} = \underbrace{-\mu_r \frac{\mu_+^2}{d^3} \sum_{k=1}^{N-1} \frac{N-k}{k^3}}_{E_{+-}} + \underbrace{\frac{1+\mu_r^2}{2} \frac{\mu_+^2}{d^3} \sum_{k=2}^{N-2} \frac{N-k}{k^3}}_{E_{--}+E_{++}}, \tag{6}$$

where the dipole moment μ_+ is assumed to be fixed, furthermore, in the first and the second term the summation is restricted to odd, and even values of k, respectively. In Eq. (6) the first term E_{+-} denotes the interaction energy of different types of particles, while the second one is the sum of the interaction energies of the same type of particles $E_{++} + E_{--}$. In the special case of $\mu_r = 1$, when oppositely oriented dipoles have the same magnitude Eq. (6) simplifies to the form

$$\begin{aligned} E_{ch} &= \underbrace{-\frac{\mu_+^2}{d^3} \sum_{k=1}^{N-1} \frac{N-k}{k^3}}_{E_{+-}} + \underbrace{\frac{\mu_+^2}{d^3} \sum_{k=2}^{N-2} \frac{N-k}{k^3}}_{E_{--}+E_{++}} \\ &= \frac{\mu_+^2}{d^3} \sum_{k=1}^{N-1} (-1)^k \frac{N-k}{k^3}. \end{aligned} \tag{7}$$

Since thermal motion is hindered by the relatively large particle mass, when a chain is formed in the colloid, it cannot reorganize itself to further decrease its energy. (The role of

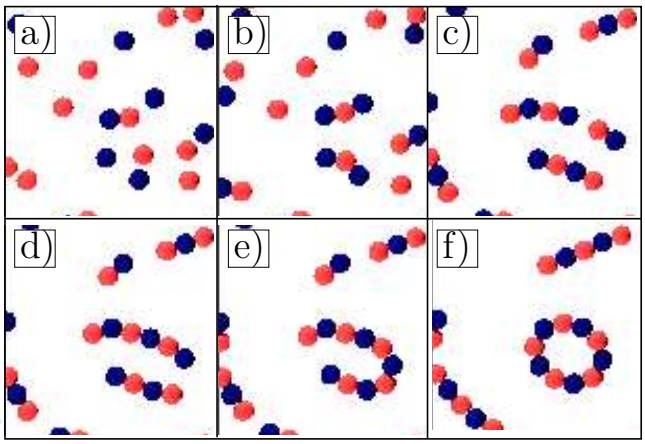

FIG. 7: Formation of a ring of alternating particles starting from a random configuration at $\mu_r = 1$, $\phi_r = 1$, and $\phi = 0.125$. Two nearby chains join and create a ring.

the Brownian motion of particles in the restructuring of colloidal aggregates has recently been demonstrated in Ref. (Chakrabarti et al. 2004) for a single component system.) When longer chains are formed by the aggregation of shorter ones, usually they undergo a straightening process until they reach the deepest energy given by Eqs. (6,7).

In order to understand the appearance of closed loops of alternating particles observed in experiments we calculated how the energy of a chain changes when it is gradually bent and finally closed to form a ring. Due to symmetry reasons a perfect regular ring can only be an equilibrium configuration when both types of particles have the same magnitude of dipole moment $\mu_r = 1$ that's why the following calculations are restricted to this case. Under the bending process the particles are assumed to lie always on a circular arc parameterized by the bending angle γ which ranges from 0 (straight chain) to 2π (closed ring). Starting from Eq. (7) the energy E_{ch} as a function of γ can be cast in the form for an even number N of particles

$$E_{ch}(\gamma) = \frac{\mu_+^2 \sin^3\left(\frac{\gamma}{2N}\right)}{d^3} \left[\sum_{k=1}^{N-1} (-1)^k \frac{N-k}{\sin^3\left(k\frac{\gamma}{2N}\right)}\right]. \qquad (8)$$

The form of $E_{ch}(\gamma)$ is illustrated in Fig. 6 for $N = 6$ where the interaction energy of identical $E_{++}(\gamma) + E_{--}(\gamma)$ and different particles $E_{+-}(\gamma)$ are also shown separately. Since during the gradual bending process the particles of the chain get closer to each other, the sum of the energies $E_{++} + E_{--}$ monotonically increases, which results in an increase of the total

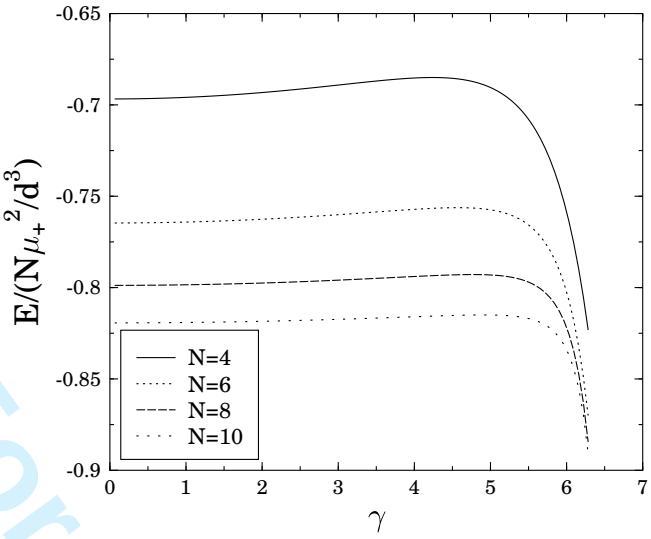

FIG. 8: Energy divided by the number of particles of a bent chain for $N = 4, 6, 8, 10$. $E_{ch}(\gamma = 0)$ and $E_{ch}(\gamma = 2\pi)$ provide the energy of a straight chain and a perfect ring, respectively.

energy E_{ch}. However, the interaction energy E_{+-} of different particles is a monotonically decreasing function of γ which can overweight the repulsion of identical particles when surpassing a certain bending angle making the closed ring to be energetically favorable for the particle system. It follows from the above argument that a chain of an even number of particles cannot spontaneously close to form a ring due to the energy barrier. Instead, rings emerge starting from a random configuration by aggregation of nearby chains formed with appropriate orientation as it is demonstrated by Fig. 7. Fig. 8 illustrates the energy of bent chains as a function of γ for various number of particles N. It can be observed in the figure that the energy barrier for bending and the difference of the chain and ring energies, *i.e.*, the difference of $E_{ch}(\gamma = 0)$ and $E_{ch}(\gamma = 2\pi)$, decrease with increasing N. Comparing chain and ring energies in Fig. 9 in a broad range of N, it can be seen that the difference decreases with increasing N and it disappears in the limit of large N.

When increasing μ_r in the model starting from a regular ring at $\mu_r = 1$, the ring structure gets distorted because particles of the larger dipole moment tend to increase their distance. At any value of μ_r both types of particles lie always on a circle, however, the radius is larger for particles of the larger dipole moment. Finally, the structure ends up in a regular polygon of corner number $N/2$, where particles of the larger moment are located in the corners, and

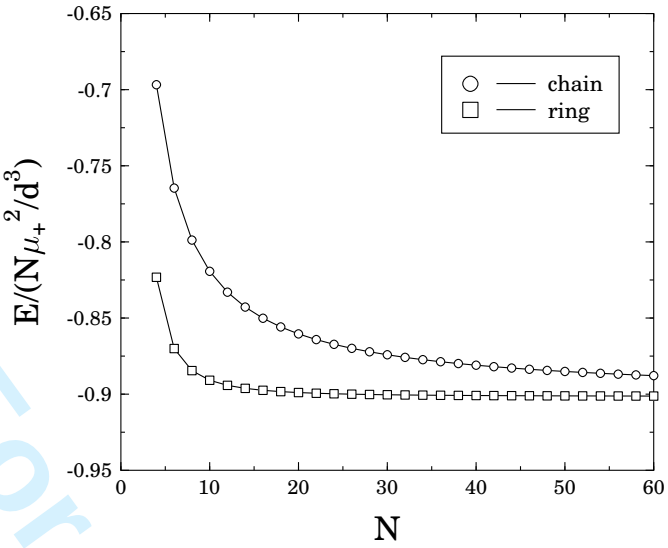

FIG. 9: Comparison of the energy of chains and rings of even number of particles as a function of the particle number N.

the smaller ones are in the middle of the sides of the polygon. The transformation of a regular ring into a regular polygon of alternating particles is demonstrated by Fig. 10.

Increasing the relative dipole moment μ_r further the polygon structure suddenly opens up into a straight chain or breaks up into short chains. It follows from our calculations that the closed loops of particles observed in the experiments (Ristenpart et al. 2003) must attain a spatial structure between the perfect ring and polygon conformations. Since closed loops (distorted rings) emerge by the aggregation of appropriately oriented nearby chains and only in the case of even number of particles, it is a rather rare event depending also on the concentration. Simulations showed that they most frequently occur at concentrations $\phi \approx 0.125$ with $\phi_r = 1$, and $\mu_r = 1$.

VI. STRUCTURE OF GROWING AGGREGATES

In order to explore the structural properties of binary colloids, simulations have been carried out varying the three parameters of the model ϕ, ϕ_r and μ_r in a broad range. Figure 11 shows simulation results obtained at different concentrations ϕ and relative dipole moments μ_r, fixing the relative concentration $\phi_r = 1$. It can be seen that at low concentrations the particles undergo a kinetic aggregation process and form chains and rings of alternating

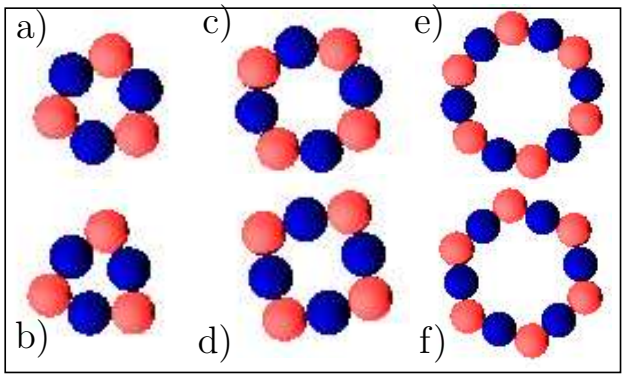

FIG. 10: Transformation of regular rings (upper row) of alternating particles into regular polygons (lower row) when increasing the relative dipole moment starting from $\mu_r = 1$ for $a, b)$ $N = 6$, $c, d)$ $N = 8$, and $e, f)$ $N = 12$.

types of particles due to the attractive interaction of oppositely directed dipoles (Fig. 11a and c).

At low concentrations the chain is the dominating morphology since due to the hindered thermal motion their is no possibility of relaxation towards more compact cluster shapes of deeper energy. The length of alternating chains is limited, when the chain length becomes comparable to the average distance of chains, aggregation can occur not only at chain ends but also at internal particles resulting in branching and more compact structures. In the simulations the time evolution of the system was followed until percolation occurred, *i.e.,* a spanning cluster connecting two opposite sides of the simulation box was formed.

In order to characterize the structure of growing clusters we calculated the radius of gyration

$$R_g^2(n) = \frac{1}{n(n-1)} \sum_{i \neq j=1}^{n} (\vec{r}_i - \vec{r}_j)^2 \tag{9}$$

for each cluster during the time evolution of the system and averaged over clusters of the same size n. In Eq. (9) $\vec{r}_i$ denotes the position of particle i in the cluster. In Fig. 12 the cluster size n is plotted as a function of the averaged gyration radius R_g on a double logarithmic plot for several different concentrations. It can be observed in the figure that for each concentration $n(R_g)$ is composed of two distinct parts of power law functional form

$$n \sim R_g^D \tag{10}$$

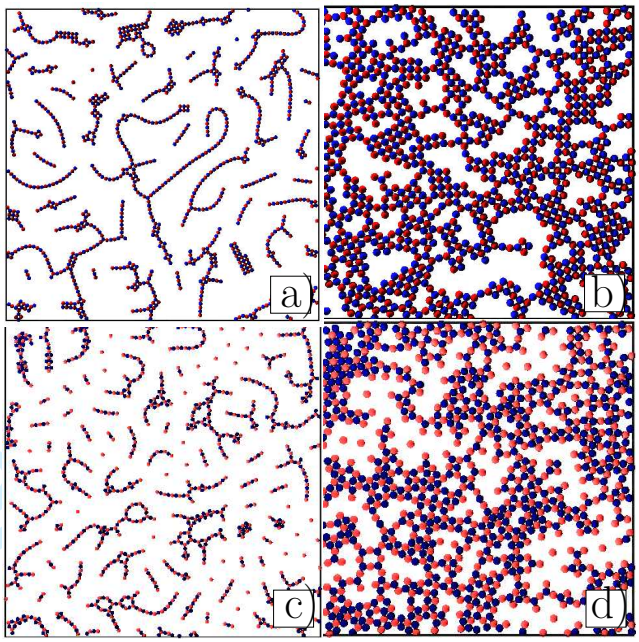

FIG. 11: The aggregation of dipoles with fixed $\phi_r = 1$, at different concentrations and relative dipole moments: *a*) $\phi = 0.125$, $\mu_r = 1$, *b*) $\phi = 0.5$, $\mu_r = 1$, *c*) $\phi = 0.125$, $\mu_r = 2.5$, and *d*), $\phi = 0.50$, $\mu_r = 2.5$.

i.e., for small clusters $n(R_g)$ can be well fitted by a power law of an exponent close to 1 indicating chainlike structures. At a certain chain length $n_c(\phi)$ depending on the concentration ϕ, however, a crossover occurs into a more compact structure characterized by a higher exponent of R_g, $D = 1.45 \pm 0.05$ was determined from simulations for $\mu_r = 1$ and $\phi_r = 1$. It follows from our argument that the crossover chain length n_c has a power law dependence on the concentration $n_c \sim \phi^{-\beta}$ with an exponent $\beta = 1.0$. The numerical result is presented in the inset of Fig. 12 where $\beta = 1.18 \pm 0.05$ was obtained in a reasonable agreement with the analytic prediction.

Simulations revealed that the aggregation process and the exponent D characterizing the structure of growing aggregates do not change until $\phi < \phi^* \approx 0.25$. However, the value of the relative dipole moment μ_r has a substantial effect on the aggregation process. It can be seen in Fig. 11*c* that at the higher value of μ_r more compact aggregates occur, *i.e.,* they are more branched and less elongated characterized by a larger value of the fractal dimension D showing a crossover from $D = 1.1 \pm 0.05$ to $D = 1.65 \pm 0.07$ when increasing the concentration ϕ at the fixed $\phi_r = 1$. Increasing the concentration above ϕ^* the morphology of clusters

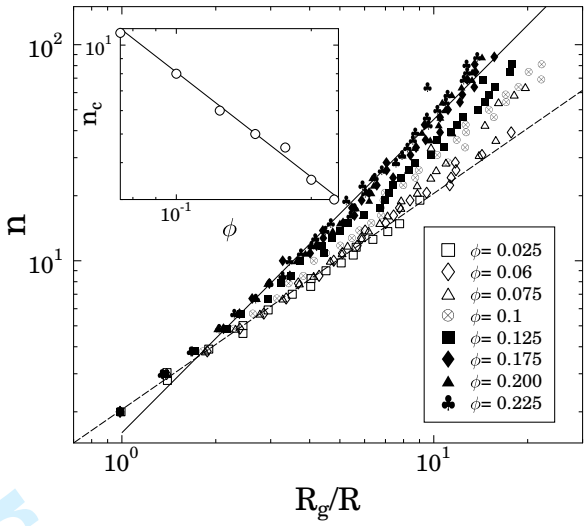

FIG. 12: The number of particles n of clusters as a function of the radius of gyration R_g. The dashed and continuous straight lines have slope 1 and 1.45, respectively. The crossover value n_c was obtained as the crossing point of the straight lines fitted to the two regimes of different slopes. The inset shows $n_c(\phi)$ where a straight line of slope 1.18 ± 0.05 was fitted to the data.

changes drastically; crystallites of various lattice structures are formed which then aggregate into large clusters as in Figs. 11b, d, where a network of crystallites can be observed. At even higher concentrations the entire system self assembles into a crystalline lattice of alternating particles.

VII. CRYSTALLIZATION

In the previous section we have shown that at high concentrations, instead of chains, rings and fractal aggregates, the particles rapidly form closed packed compact islands with crystalline order in the colloid. Computer simulations performed in the high concentration phase varying the relative concentration ϕ_r and the relative dipole moment μ_r of the components showed that various crystalline morphologies can be obtained in certain parameter regimes. In order to understand the formation of crystal structures in binary colloids and explore possible lattice morphologies, we calculated the energy of basic particle configurations from which lattices can be built up. The Basic Configurations (BC) are composed of a particle of type I (with dipole moment μ_+) surrounded by 2 (BCI), 3 ($BCII$), 4 ($BCIII$), 5 ($BCIV$),

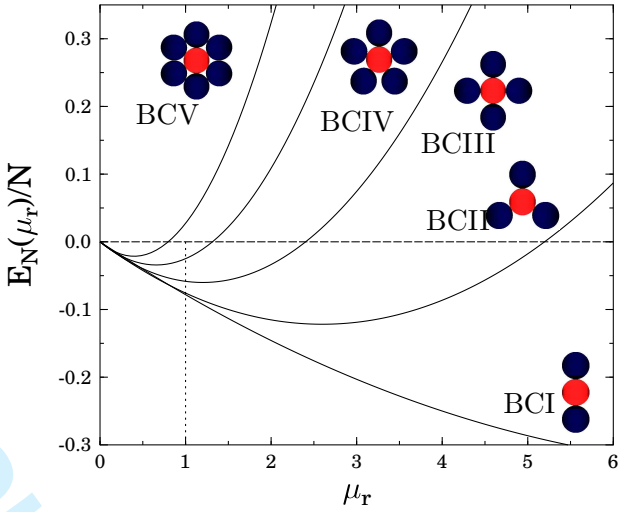

FIG. 13: The energy Eq. (11) divided by the number of particles of elementary particle configurations as a function of μ_r for $N = 3, 4, 5, 6, 7$. For clarity, the corresponding particle configurations are also presented.

or 6 (BCV) particles of type II (with dipole moment μ_-) placed at the energetically most favorable locations. In order to simply cover also cases where the different types of particles are interchanged, the energy of BCs was calculated as a function of $\mu_r = \mu_-/\mu_+$ fixing the value of $\mu_+ = 1$

$$E_N(\mu_r) = \frac{\mu_+^2}{d^3}\left[\frac{\mu_r^2}{8}\sum_{k=1}^{N-2}\frac{N-k-1}{\sin^3(k\beta)} - \mu_r(N-1)\right], \tag{11}$$

where $\beta = \pi/(N-1)$ and the particle number takes the values $N = 3, 4, 5, 6, 7$. The energy divided by the particle number $E_N(\mu_r)/N$ is presented in Fig. 13 as a function of μ_r for the possible values of N. It can be seen in the figure that all the BCs are stable (have a negative energy) only in certain μ_r ranges between 0 and an upper bound $\mu_r^{max}(N)$ since with increasing μ_r the attraction exerted by the central particle is not enough to compensate the mutual repulsion of the surrounding ones. Such configurations where the central particle is surrounded by particles of smaller dipole moment, *i.e.* $\mu_r < 1$ in Fig. 13, are always stable except for BCV because $\mu_r^{max}(7) \approx 0.8$ falls below 1. The upper bounds can be determined exactly from Eq. (11) as $\mu_r^{max}(N) \approx 16, 5.2, 2.4, 1.3, 0.8$ was obtained for $N = 3, 4, 5, 6, 7$, respectively.

Repeating the above basic structures with alternating particles various structures can

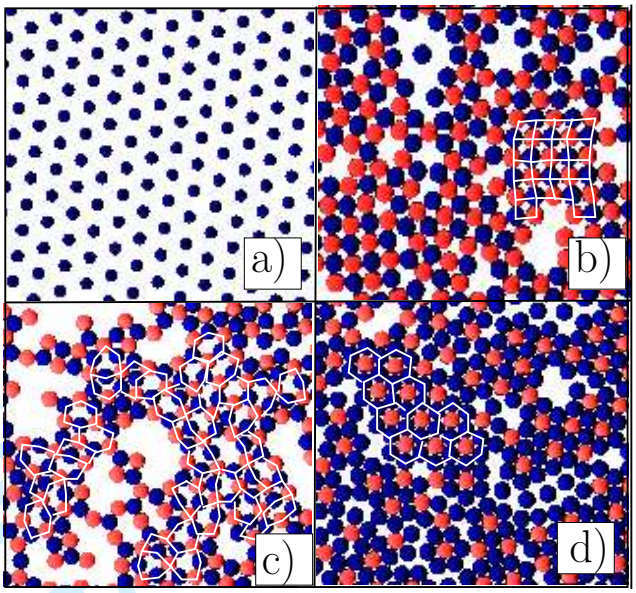

FIG. 14: Crystalline morphologies obtained by simulations. In each system 1000 particles were used and the concentration was controlled by changing the size of the simulation box. For visualization smaller pieces of the simulation box are cut out and magnified.

be built up, *i.e.* BCI results in chains or rings, $BCII$ gives rise to a honeycomb lattice in which both types of particles have three neighbors of the other type, and $BCIII$ leads to the square lattice. $BCIV$ can result in quasi-crystalline structure with local five fold symmetry (Wen and Sheng 2003, Wen et al. 2000). Moreover, BCV forms the basis of the binary Hexagonal Closed Packed structure, in which particles of the larger dipole moment have 6 neighbors of the smaller one but particles of the smaller moment have 3 neighbors of both types. The overall morphology attained by the entire particle system at a given value of μ_r is not necessarily based on the energetically most favorable basic configuration. In spite of the isotropic particle-particle interaction the cluster-cluster interaction is highly anisotropic which can result in trapping the particles into local energy minima in configuration space, especially when thermal motion is hindered by the relatively large particle mass. Hence, the relative dipole moment μ_r, the total concentration ϕ and the relative concentration ϕ_r of components together determine the final structure. Based on the energy of basic configurations Eq. (11) and Fig. 13, it is possible to determine analytically regions of ϕ, ϕ_r, and μ_r, which are needed to obtain a certain lattice structure or aggregate morphology.

Figs. 14, 15 provide an overview of possible structures obtained by simulations varying

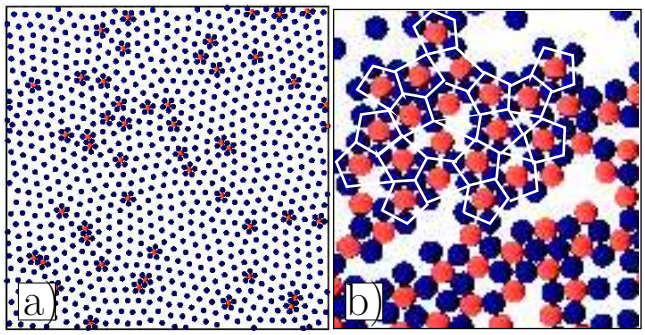

FIG. 15: *a*) Flower-like binary islands in a triangular lattice ($\phi = 0.4$, $\phi_r = 5$, $\mu_r = 2.0$), *b*) quasi-crystalline structure with local five-fold symmetry ($\phi = 0.66$, $\phi_r = 2$, $\mu_r = 1.8$).

ϕ, ϕ_r, μ_r. If one of the components has a much larger concentration than the other one (for instance, $\phi_+ >> \phi_-$), due to the repulsive interaction of the identical particles a triangular lattice is formed with some binary islands. The limiting case when only one of the components is present is shown in Fig. 14*a* where a regular triangular lattice is observed. Gradually adding particles of the other type to the system first flower-like islands of the form of the basic configurations BCIV and BCV occur. It can bee seen in Fig. 15a that far from these island the triangular structure of the original lattice restores.

The simplest basic configuration BCI gives rise to chain and ring conformations which occurs at $\mu_r = 1, \phi_r = 1$, in the concentration range $\phi < 0.12$. At concentrations $0.12 < \phi < 0.25$ fractal structures were obtained as discussed earlier. Chains and rings emerge, of course, in a broader interval of μ_r and ϕ_r but the unit values proved to be the most advantages. Simulations revealed that rings appear when two nearby chains merge which occur most frequently at concentrations $\phi \approx 0.125$, see Figs. 7*a*, *c*).

At high concentrations lattice structures can be obtained, however, concentrations too close to the highest coverage ($\phi \approx 0.9$) are disadvantages because they prevent particle motion and result in freezing into local energy minima. Hence, the best square lattice structures can be achieved at $\phi \approx 0.65 - 0.75$. This type of lattice contains the same amount of both type of particles so that $\phi_r = 1$ and $\mu_r = 1$ follows, see Fig. 14*b*. The parameter regime providing square lattice agrees well with our experimental observations and of that of Ref. (Ristenpart et al. 2003). The binary honeycomb lattice where each particle has 3 neighbors of the other type has not been observed experimentally in Ref. (Ristenpart et al. 2003) where the particle monolayer was subjected to an AC electric field.

In our experiments, however, the honeycomb structure naturally occurred in a quite broad parameter range. An example of the binary honeycomb lattice is presented in Fig. 14*c* which was obtained by computer simulations at $\phi = 0.5$ and $\phi_r = 1$. For clarity, some plaquettes of the lattice are highlited in the figure. The basis of this structure is $BCII$ which is always stable for $\mu_r < 1$, *i.e.* when a larger dipole is surrounded by 3 smaller ones. However, to make the opposite configuration more favorable, μ_r has to be increased above the stability limit of $BCIII$ (above $\mu_r^{max}(5) \approx 2.4$), otherwise, the system ends up in a square packed structure. $\mu_r \approx 2.5$ proved to be an excellent choice numerically, see Fig. 14*c*.

If the magnitude of the two dipole moments are different ($\mu_r \neq 1$) concentration fluctuations easily lead to the formation of the hexagonal-closed-packed structure, where particles of the larger dipole moment have 6 neighbors of the other type and the ones with smaller dipole moment have 3 of both types. The highest portion of the system was found to crystallize into HCP structure at $\phi \approx 0.80 - 0.82$ with the ratio of $\phi_r = 2$ of the components and with high enough asymmetry of the magnitude of dipole moments $\mu_r \approx 2.5$, which is needed to prevent the system to crystallize locally into the square packed structure. The corresponding simulation results can be seen in Fig. 14*d*, which is in a nice agreement with our experiments.

If the relative dipole moment favors the formation of $BCIV$, no crystal structure can occur, however, quasi-crystalline ordering can be obtained with local five-fold symmetry, as it is illustrated in Fig. 15b.

If the relative dipole moment μ_r is even higher ($\mu_r > 2.5$) but the concentration and the relative concentration do not favor the emergence of the HCP lattice, so-called super structures can be observed in the colloid. These structures do not have ordered crystalline morphology, instead they are characterized by long straight binary chains which connect disordered or small crystalline island as in Figs. 11*b*, *d*.

VIII. CONCLUSIONS

A detailed experimental and theoretical study of the structure formation in a binary dipolar monolayer was presented. We constructed an experimental technique which provides a straightforward and controllable realization of binary monolayers with particles of oppositely oriented dipole moments constrained to be perpendicular to the plane of motion. In the ex-

perimental setup, macroscopic particles are constructed by attaching particles of permanent magnetic moment to swimmers. The swimmers have two roles in the experimental setup, *i.e* they ensure the confinement of the composite particles to the air-water interface (floating), and prevent flipping, constraining the dipole moment of the particles perpendicular to the water surface. One of the main advantages of the experimental setup is that it does not require external fields to generate particles of different dipole moments, which also leads to a substantial simplification of the dynamics of the particle system. However, the magnitude of the dipole moment, and hence, the strength of interaction of the components cannot be continuously modulated. Experiments were performed varying the total concentration of the particles, furthermore, the relative concentration and relative dipole moment of the components. At low concentrations, cluster-cluster aggregation was observed with chain-like morphologies, while at higher concentrations a diverse assortment of planar crystal lattices was obtained: the particles formed triangular lattices of a single component, furthermore, binary honeycomb and square lattices, and hexagonal closed packed structures.

We constructed a two-dimensional dynamical model of binary monolayers by considering solely the dipole-dipole interaction of particles and Stockes drag exerted by the liquid on the particles. Varying the three parameters of the model, *i.e.* the total concentration of the particles ϕ, the relative concentration ϕ_r and the relative dipole moment μ_r of the components a rich variety of structures were obtained in satisfactory agreement with the experimental findings. At low concentrations kinetic aggregation occurs which results in chains of alternating particles. Under appropriate conditions nearby chains can merge to form rings or polygons achieving a deeper energy. The length of chains is limited, at a critical chain length a crossover occurs to fractal aggregates characterized by the fractal dimension, which depends on the relative dipole moment of the components. The crossover length has a power law dependence on the concentration of the particles.

In the high concentration phase the particles self organize into crystalline morphologies of various types, *i.e.*, depending on the relative concentration and relative dipole moment of the particles, a triangular lattice, a square lattice, honeycomb and HCP structures can be formed, furthermore, quasi-crystalline structure with local five fold symmetry can be obtained. We determined the parameter regimes of the occurrence of crystal and quasi-crystal structures in a good agreement with experiments. The simplicity of the model demonstrates that the main qualitative features of the structure formation in this system

are determined by the induced dipole-dipole interaction.

Acknowledgments

This work was supported by the projects OTKA T037212 and M041537. F. Kun was supported by the György Békési Foundation of the Hungarian Academy of Sciences.

Allen, M. P. and Tildesley, D. J., 1994, *Computer Simulation of Liquids*, (Clarendon Press, Oxford).

Blair, D. L. and Kudrolli, A., 2003, Phys. Rev. E **67**, 021302.

Cernák, J., Helgesen, G., and Skjeltorp, A. T., 2004, Phys. Rev. E **70**, 031504.

Chakrabarti, A., Fry, D., and Sorensen, C. M., 2004, Phys. Rev. E **69**, 031408.

Choi, Y., Kim, K., and Pak, H. K., 2000, Physica A **281**, 99.

Froltsov, V. A., Blaak, R., Likos, C. N., and Löwen, H., 2003, Phys. Rev. E **68**, 061406.

Furst, E. M. and Gast, A. P., 1999, Phys. Rev. Lett. **82**, 4130.

Furst, E. M. and Gast, A. P., 2000, Phys. Rev. E **61**, 6732.

Ghazali, A. and Lévy, J. C., 2003, Phys. Rev. B **67**, 064409.

Grzybowski, B. A., Jiang, X., Stone, H. A., and Whitesides, W. A., 2004, Phys. Rev. E **64**, 011603.

Helseth, L. E. and Fischer, T. M., 2003, Phys. Rev. E **68**, 051403.

Huang, J. Y. and Lai, P. Y., 2000, Physica **A281**, 105.

Kun, F., Pál, K. F., Wen, W., and Tu, K. N., 2000, Phys. Lett. A**277**, 287.

Luding, S., 1998, *Collisions and contact between two particles*, in Herrmann, H. J., Hovi, J. P., and Luding, S. (eds), 1998, *Physics of dry granular media*, NATO-ASI Series (Kluwer Academic Publishers, Dordrecht).

Morimoto, H., Maekawa, T., and Matsumoto, Y., 2003, Phys. Rev. E **68**, 061505.

Ristenpart, W. D., Aksay, I. A., and Saville, D. A., 2003, Phys. Rev. Lett. **90**, 128303.

Sapozhnikov, M. V., Tolmachev, Y. V., Aranson, I. S., and Kwok, W. K., 2003, Phys. Rev. Lett. **90**, 114301.

Skjeltorp, A. T., 1983, Phys. Rev. Lett. **51**, 2306.

Strambaugh, J., Lathrop, D. P., Ott, E., and Losert, W., 2003, Phys. Rev. E **68**, 026207.

Tavares, J. M., Weis, J. J., and da Gamma, M. M. T., 2002, Phys. Rev. E **65**, 061201.

Teixeira, P. I. C., Tavares J. M., and da Gama, M. M. T., 2000, J. Phys.: Condens. Matter **12**, R411.

Terada, Y. and Tokuyama, M., 2004, Physica A **334**, 327.

Varga, I., Kun, F., and Pál, K. F., 2004, Phys. Rev. E **69**, 030501(R).

Vicsek, T. and Family, F., 1984, Phys. Rev. Lett. **52**, 1669.

Weis, J. J., 2002, Mol. Phys. **100**, 579.

Weis, J. J., Tavares, J. M., and da Gamma, M. M. T., 2002, J. Phys.: Condens. Matter **14**, 9171.

Wen, W. and Sheng, P., 2003, Physica B **338**, 343.

Wen, W., Kun, F., Pál, K. F., Zheng, D. W., and Tu, K. N., 1999, Phys. Rev. E **59**, R4758.

Wen, W., Zhang, L., and Sheng, P., 2000, Phys. Rev. Lett. **85**, 5464.

Yeh, S., Seul, M., Shralman, B. L., 1997, Nature **386**, 57.

Yoshioka, N. et al., 2005, unpublished.

Zahn, K., Wille, A., Maret, G., Sengupta, S., and Nielaba, P., 2003, Phys. Rev. Lett. **90**, 155506.